Studies of the Polymerization of Methacrylic Acid via Free-Radical Retrograde Precipitation Polymerization Process

ANUJ AGGARWAL,[1] RAHUL SAXENA,[1] BO WANG,[2] and GERARD T. CANEBA[1,*]

[1]Department of Chemical Engineering, Michigan Technological University, Houghton, Michigan 49931, and
[2]Department of Chemistry, Michigan Technological University, Houghton, Michigan 49931

SYNOPSIS

In this paper, we present some new results of our work in a novel polymerization process (called the free-radical retrograde precipitation polymerization, or FRRPP, process) that occurs at temperatures above the lower critical solution temperature. Our polymerization experiments basically involve the methacrylic acid–poly(methacrylic acid)–water system. Experimental results indicate a gradual increase in conversion with time after what seemingly is the onset of phase separation. In an equivalent solution polymerization system, conversion of methacrylic acid reaches almost 100% at a much shorter time than in the FRRPP system. Molecular weights of poly(methacrylic acid) at different times for the FRRPP system are not dramatically different from those obtained in the solution system. However, the FRRPP system yields a relatively narrow molecular weight distribution at a wide range of conversion compared to that obtained in the equivalent solution system. The unique characteristics of the FRRPP process is shown in the asymptotic time behavior of the free-radical concentration compared to the decay behavior in other polymerization systems. © 1996 John Wiley & Sons, Inc.

INTRODUCTION

Within the past several years, we have been studying the physico-chemical and product material aspects of a free-radical precipitation polymerization reaction systems wherein phase separation occurs above the lower critical solution temperature (LCST).[1] In contrast with conventional precipitation polymerization (CPP) process[2–5] that involves phase separation below the upper critical solution temperature (UCST). We call this new process a free-radical retrograde precipitation polymerization (FRRPP) process (see Fig. 1). The added complication of retrograde precipitation could be offset by tighter control of reactor operating conditions and polymer molecular properties. Also, the relatively low operating pressures typically needed are not of great economic disadvantage inasmuch as commercial implementation can be effected using typical commercial autoclave polymerization reactors. In fact, this work involves a system that has been shown to undergo retrograde precipitation polymerization in an atmospheric reactor system.

From an earlier work,[1] we proposed the following features of the FRRPP process:

1) gradual increase of conversion versus time even under gel effect conditions;
2) local heating around the radical site;
3) reduced rate of propagation, as well as the rate of radical-radical termination;
4) relatively narrow molecular weight distributions; and
5) the existence of live radicals that could be exploited for production of block copolymers.

In an experiment involving a polystyrene–styrene–ether system, we were able to indirectly observe the possible occurrence of hot spots in the reactor fluid. Also, the product polymer had a narrow molecular

* To whom correspondence should be addressed.

Journal of Applied Polymer Science, Vol. 62, 2039–2051 (1996)
 CCC 0021-8995/96/122039-13

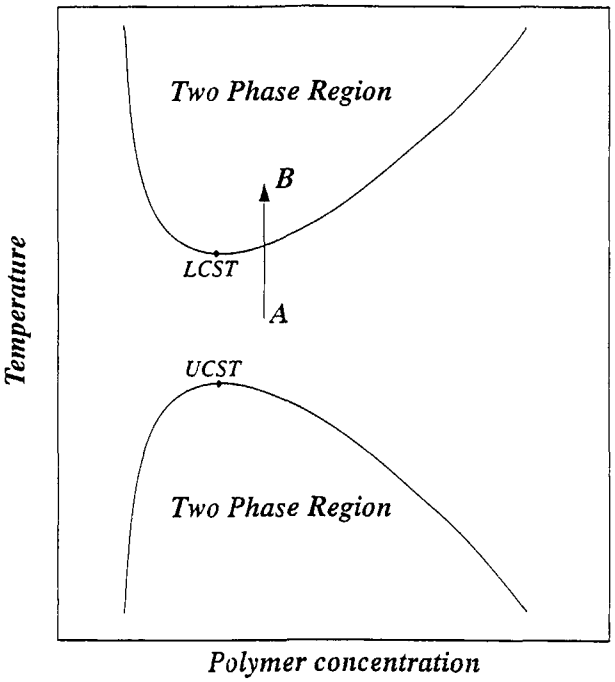

Figure 1 Binary phase diagram for a typical amorphous polymer–solvent system showing phase curves for conventional (temperature below the UCST) and retrograde (temperature above the LCST) precipitation processes. Retrograde precipitation would involve going from point A to B.

weight distribution. A second experiment involving the polystyrene–styrene–acetone system showed that at the beginning of the polymerization process, there was an accumulation of polymer with almost the same molecular weight and the same polydispersity index of 1.4. In the next experiment involving the same Polystyrene/Styrene/Acetone system, an increase in average molecular weight was observed long after almost all the initiator molecules have decomposed. Also, the results suggested a gradual increase in conversion vs. time. Finally, an experiment was done to make a block copolymer (which was believed to contain PMMA-PBA-PMMA triblock copolymer due to existence of rubbery plateau in a dynamic mechanical analyzer) through the sequential addition of monomers.

In this paper, we present results of the polymerization of methacrylic acid, indicating a relatively gradual conversion rate after what is seemingly the onset of phase separation. We also show evidence of control of molecular weight and molecular weight distribution. Comparison of the FRRPP behavior is made with equivalent conventional precipitation, solution, and bulk polymerization systems. We also show nuclear magnetic resonance (NMR) spectroscopy results for the product poly(methacrylic acid), which indicates random tacticity behavior for both solution- and FRRPP-synthesized products. Finally, results of turbidity and time-resolved light scattering experiments support the proposition that phase separation occurs during the polymerization of methacrylic acid in water above the lower critical solution temperature.

EXPERIMENTAL

Polymerization Experiments

The monomer used in this work, methacrylic acid, was purchased from Aldrich Corporation. Other fluids used were analytical grade DMF, mixed xylenes, and water. Initiators used were AIBN (from Eastman Kodak Co.) and V-50 (which contains 98.8% 2,2′-Azobis(2-amidonopropane)-dihydrochloride, from Wako Chemical Co.), while Span 20 (sorbitan monolaurate from Aldrich Corporation) was used as surfactant. The monomer and other reactor fluids were distilled and bubbled with nitrogen gas (with less than 2 ppm oxygen content) for at least 15 min before they were used in the experiments. The initiator and surfactant were used as is.

The reactor system used in the polymerization of methacrylic acid was a typical 500 mL atmospheric reactor system under a slight nitrogen gas pressure (Fig. 2). In this experiment, the reacting system (methacrylic acid, water, poly(methacrylic acid), and V-50) was dispersed in mixed xylenes with the aid of the surfactant (Span 20). This assures the minimal scale formation in the reactor and a reliable sampling of the reactor fluid. A typical experiment began with charging the following into the 500 mL reactor: 17.25 g Span 20, 12.18 g methacrylic acid, 110 g water, and 195.75 g mixed xylenes. The mixture was heated to 80°C under a nitrogen blanket. Note that the lower critical solution temperature of poly(methacrylic acid)–water system is at about 50°C.[6,7] The initiator (0.06 g of V-50) was dissolved in 10 g of water at room temperature and then charged into the reactor. Liquid samples of known weight were withdrawn from the reactor at definite time intervals, cooled in an icebath, and purged with air to freeze the reaction. At the end of the polymerization experiment, the liquid samples and the remaining fluid in the reactor were all weighed. Very little unaccountable loss of reactor fluid was observed, and such loss was reflected as part of uncertainty in the data.

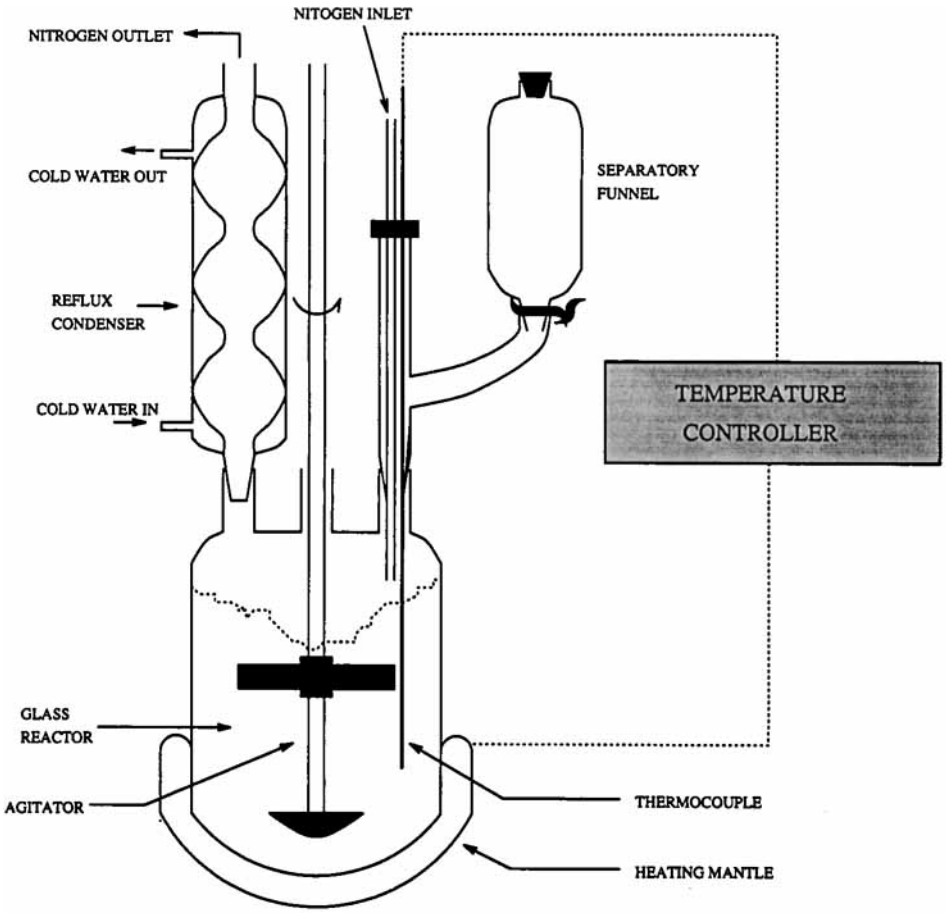

Figure 2 Atmospheric polymerization reactor system used in this work.

The liquid samples taken from the reactor were dried to constant weight. The dried material was ground in a mortar and pestle and washed with analytical grade isopropyl alcohol five to six times to extract the surfactant and unreacted monomer. The grinding process is not believed to affect the molecular weight distribution to any significant amount for two reasons. First, sieve analyses of a number of ground samples revealed that about 26% passed through a 26 μm screen and that particle size distributions are unimodal with about 60% of particle weight between 37 and 125 μm. Second, particles in the reactor are of emulsion sizes in the order of 0.1 μm, and they will be coated with surfactant molecules. Thus, grinding will most likely be breaking up agglomerated particles from the reactor; this, of course, is not likely to result in breakage of individual particles. The insolubility of poly(methacrylic acid) in isopropyl alcohol has been reported,[8] and the solubility of the surfactant and monomer was verified experimentally. The washed samples were dried and used in subsequent molecular weight and NMR analyses.

In order to establish a reference system, the same reactor conditions of monomer concentration, temperature, and initiator equivalent weight fraction (which is AIBN instead of V-50) were used in solution polymerization. Here, the solvent was DMF, which we experimentally verified to be able to dissolve the polymer at reactor concentrations. The liquid samples withdrawn from the reactor were prepared in the same way as it was done with samples withdrawn from the FRRPP reactor system.

To assure consistent results, methacrylic acid polymerization experiments (FRRPP and solution polymerization systems) were repeated, and the data averaged.

Size Exclusion Chromatography

The molecular weights of the dried polymer samples from the reactor fluid were measured using a size

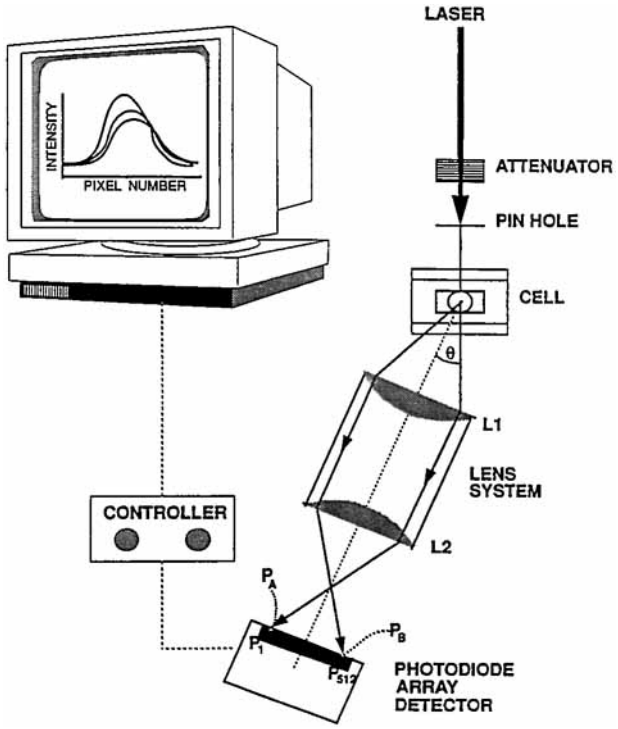

Figure 3 Schematic diagram of the light scattering system with a photodiode array detector. The polymer material system is placed in a glass container, which in turn is placed inside the optical cell. A vertically polarized He-Ne laser source is used, which is attenuated and passed through a pinhole to control its beam cross section. Scattered light is filtered by the lens system (lenses L1 and L2), which allows only scattered light from the sample to pass through.

exclusion chromatograph. The chromatography system has refractive index and multiangle light scattering detectors (Wyatt Technologies, Inc.). Thus, measured molecular weights were absolute, and there was no need to calibrate molecular weights after injecting a few samples. We used a glucose BR™ mixed bed column (Jordi Associates) with a molecular weight range of 10 to 10 million g/mol, and our carrier fluid was 80/20 v/v 0.1 NaOH solution/DMSO mixture from HPLC grade materials.

Measurements of Free-radical Concentration

In order to further differentiate the FRRPP process from other free-radical polymerization processes, we measured free-radical concentrations vs. time. For the FRRPP process, samples were withdrawn from the above-mentioned reactor system and quenched in dry ice. Then, they were freeze-dried at about −10°C under vacuum. The dried samples were transferred into 3 mm glass tubes under nitrogen gas and flame-sealed. Free radical concentrations were obtained by placing the freeze-dried products in 3 mm flame-sealed glass tubes in the sample cavity of a Varian E-109B electron paramagnetic resonance (EPR) spectrometer at room temperature. Calculation of the radical concentration was obtained by double integrating the signal and comparing the value from a calibration line using a DPPH radical standard.

For bulk and CPP processes, radical concentrations were obtained *in situ* using the Varian E-109B EPR spectrometer at 80°C. The sample solution mixture (6 g MAA, 0.048 g AIBN for the bulk system; and 6 g MAA, 0.145 g AIBN, 12 g mixed xylenes for the CPP process) was bubbled with Nitrogen gas for

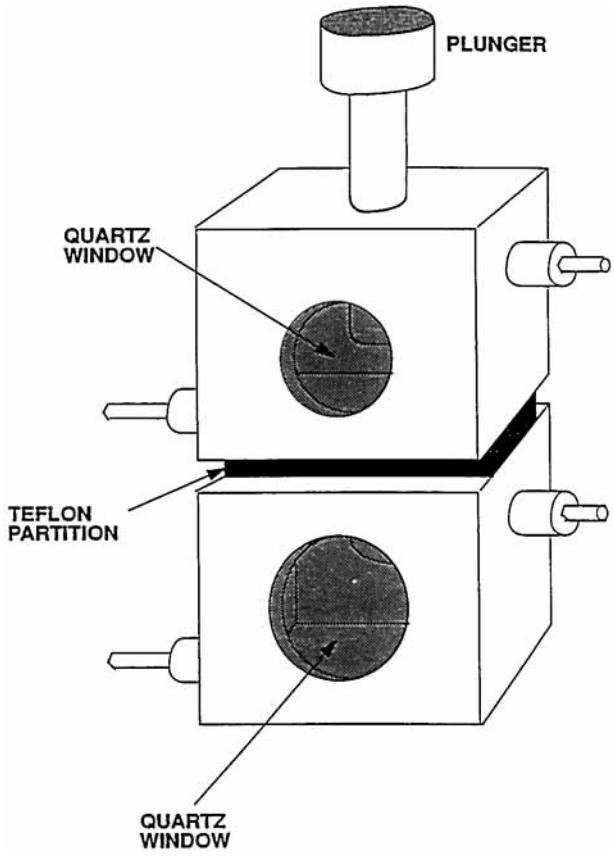

Figure 4 Outside view of the optical cell that houses the polymer system in a glass container. Glass windows are shown on two opposite sides of the cell where light goes in and out. The cell has an upper and lower chamber, which can be maintained at two different temperatures. The upper chamber is the holding compartment, while the lower chamber is heated by a flow-through fluid system at the operating temperature. At the start of the experiment, the glass container of the polymer system in the upper chamber is pushed down into the lower chamber using the plunger.

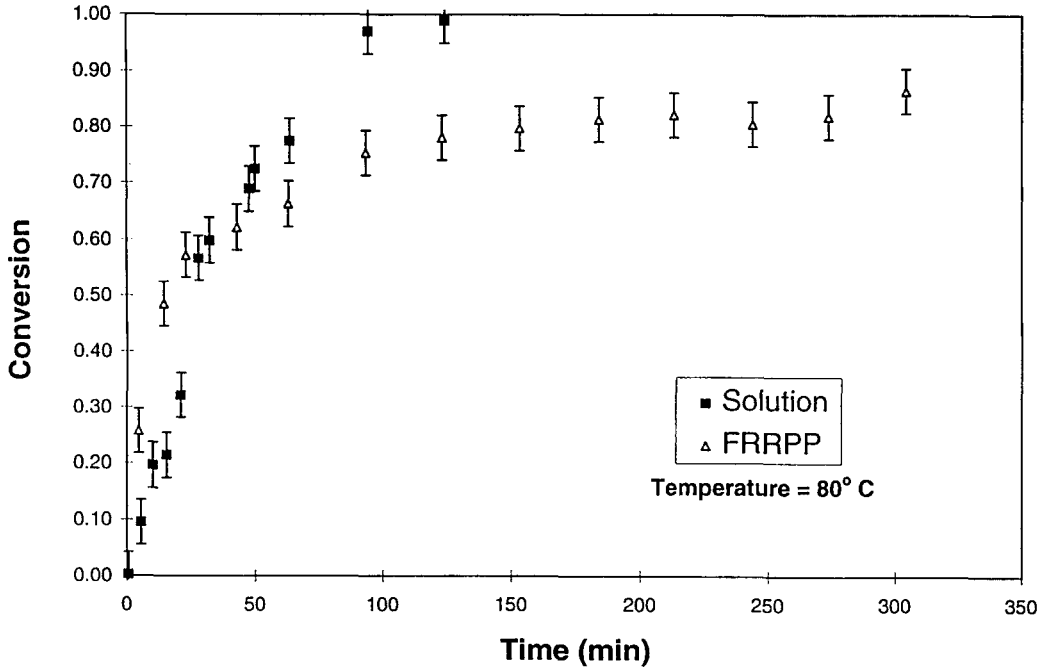

Figure 5 Conversion versus time for batch polymerization of methacrylic acid in FRRPP and solution systems at 80°C. For the FRRPP system, the reactor contained 12 g methacrylic acid, 120 g water, 0.06 g V-50, 17 g Span 20 surfactant, and 196 g mixed xylenes. For the solution system, reactor contained 32 g methacrylic acid, 320 g DMF, and 0.16 g AIBN.

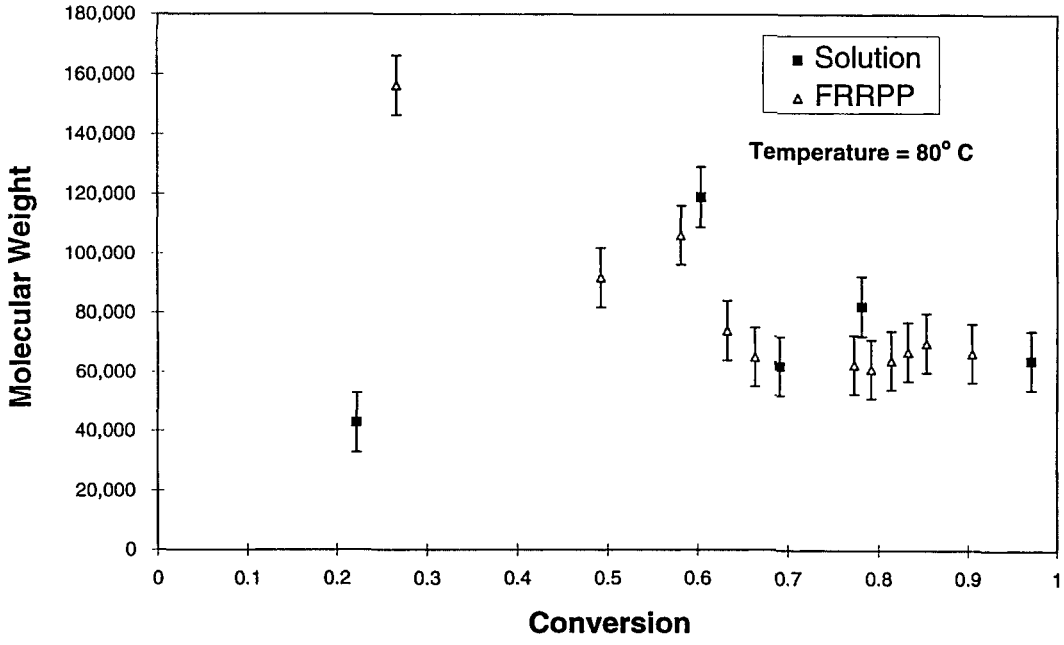

Figure 6 Number average molecular weight vs. conversion for batch polymerization of methacrylic acid at 80°C. For the FRRPP system, the reactor contained 12 g methacrylic acid, 120 g water, 0.06 g V-50, 17 g Span 20 surfactant, and 196 g mixed xylenes. For the solution system, reactor contained 32 g methacrylic acid, 320 g DMF, and 0.16 g AIBN.

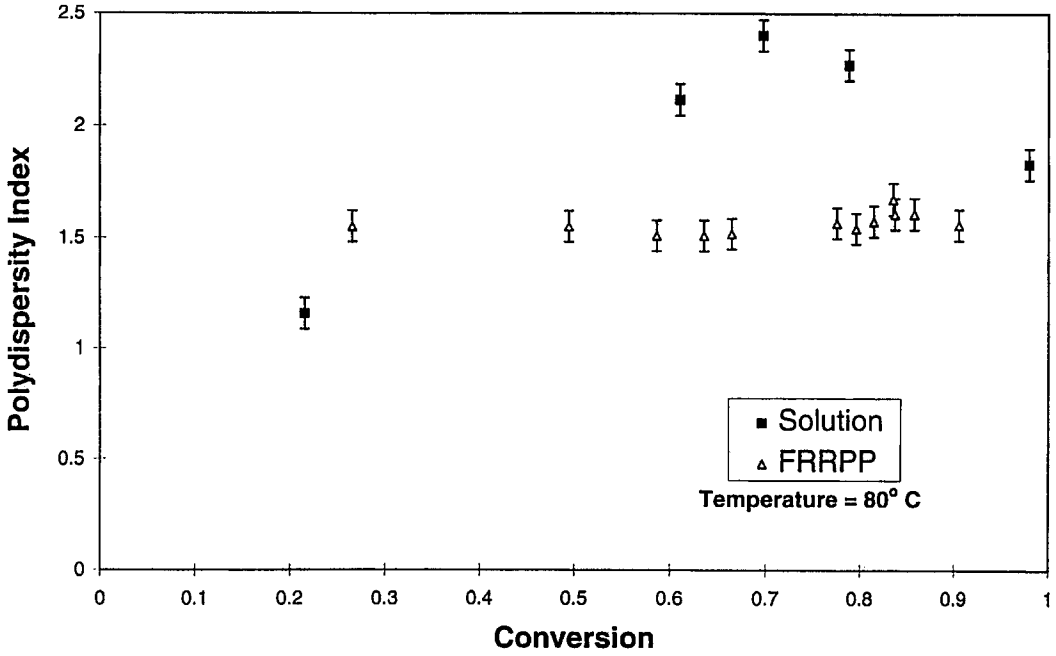

Figure 7 Polydispersity index vs. conversion for the batch polymerization of methacrylic acid at 80°C. For the FRRPP system, the reactor contained 12 g methacrylic acid, 120 g water, 0.06 g V-50, 17 g Span 20 surfactant, and 196 g mixed xylenes. For the solution system, reactor contained 32 g methacrylic acid, 320 g DMF, and 0.16 g AIBN.

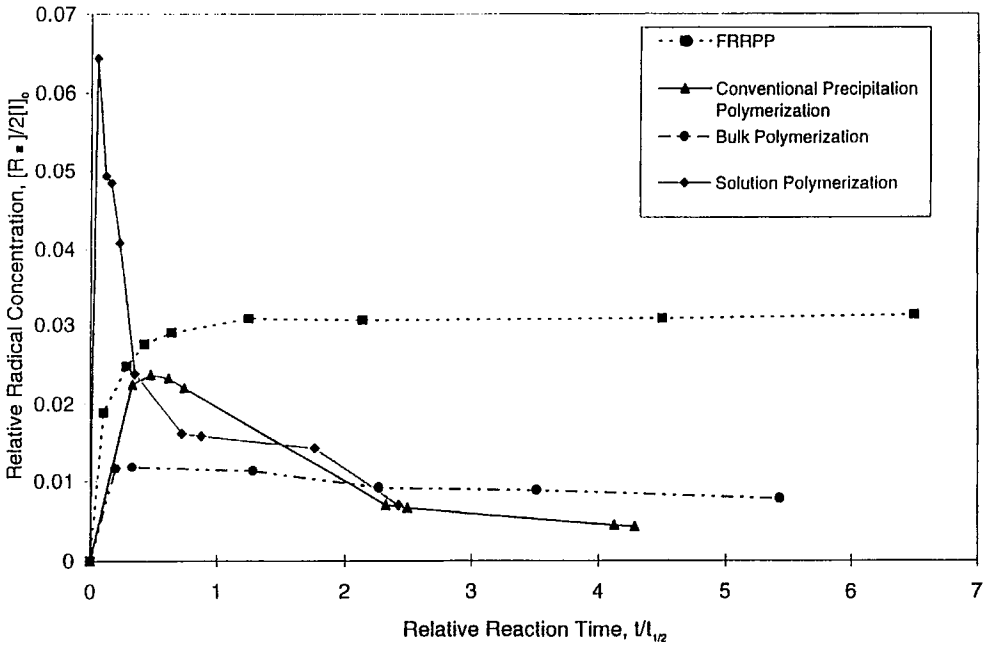

Figure 8 Comparison of evolution of experimentally measured free-radical concentrations for different modes of polymerization of methacrylic acid. Note that the radical concentration $[R^{\bullet}]$ compared to available radicals from the initiator $(2[I]_o)$ stays almost constant at a much higher value for the FRRPP process, even after five times the initiator half-life $(t_{1/2})$. Reactions were done at 80°C and at the same starting monomer composition of 10 wt %, except for the bulk polymerization process.

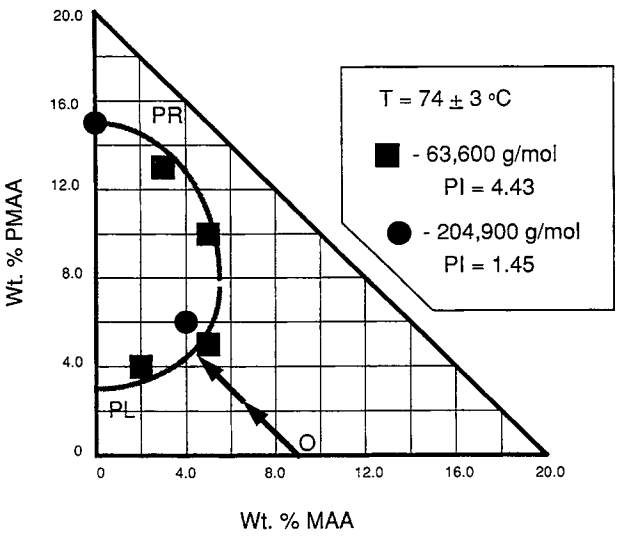

Figure 9 Ternary phase diagram for the poly(methacrylic acid)–methacrylic acid–water system for phase separation above the lower critical solution temperature. The reaction trajectory is also indicated by the arrow starting from point O. When the trajectory reaches the phase envelope, it separates into a polymer-rich (PR) phase and a polymer-lean (PL) phase.

about 5 min. Then it is charged into the EPR 3 mm sample glass tube prior to flame-sealing. The sealed tube was placed in the EPR cavity and heated to operating temperature in 1 min. The signal was obtained at different reaction times.

For the solution polymerization system, samples from the above-mentioned reactor system were withdrawn and quenched in dry ice. Known concentrations of DPPH in analytical grade toluene were added and allowed to react for 2 min. The resulting material was placed in a quartz cell and charged into a spectrophotometer for color intensity measurements. The radical concentration was obtained based on a calibration curve from color intensities of known DPPH-toluene solutions.

Nuclear Magnetic Resonance

High-resolution ^{13}C-pulsed NMR spectroscopy of product poly(methacrylic acid) was carried out using a 220 MHz Varian XL-200 NMR spectrometer. The polymer samples were dissolved in deuterium oxide (D_2O), and spectra were obtained at 80°C. In order to minimize the interference of proton signals, proton noise decoupling was applied. Spectra were obtained relative to tetramethylsilane (TMS).

Light Scattering Experiments

Light scattering experiments were carried out in order to obtain phase curve data and phase separation kinetics results. Figure 3 shows the schematic diagram of the laser light scattering apparatus used for these measurements. The intensity profile of scattered light from the sample cell was collected using the photodiode array detector (INSTASPEC Model 77140, manufactured by Oriel Corp.) consisting of 512 pixel elements. A vertically polarized He-Ne laser (wavelength of 632.8 nm) was used as incident light beam. The dual lens system allowed us to focus scattered light. Along with its blackened interior surfaces, collimated beams of scattered light were observed. The diode array detector system made it possible to measure scattering intensity at different angles almost simultaneously, thus shortening the time intervals of consecutive measurements.

The approximate ternary phase diagram was obtained using the cloud-point method. Here, known amounts of poly(methacrylic acid), methacrylic acid (analytical grade), and water (distilled) were weighed in 10 mm Pyrex™ glass tubes and vacuum-sealed. The contents of the glass tubes were tumble-mixed for one to two weeks to form a homogeneous solution. The reference scan for a homogeneous sample at room temperature was taken and subtracted from each intensity scan at various temperatures to determine the change in intensity profile with time. A tube containing a polymer solution was inserted in the sample cell (Fig. 4), and its temperature was ramped at a rate of 0.5°C per minute by a flow-through system of hot water. The point at which there is a sharp decrease in intensity at 0 degrees from the incident laser beam was noted, and the corresponding temperature determined from a strip chart recorder. This method was repeated for samples with different compositions. The compositions which exhibited turbidity at a certain temperature range correspond to points in the phase coexistence curves.

The above-mentioned light scattering system was also used for *in situ* polymerization of methacrylic acid in water with V-50 as initiator. Again, the reaction fluids were purged with nitrogen for 15 min before charging into a closed-bottom 4-mm Pyrex™ glass tube. The V-50 powder was poured into the tube. The vapor space of the tube was flushed with nitrogen before immersion of the tube in liquid nitrogen. The inside of the tube was evacuated, and the top was flame-sealed. The sealed glass tube was allowed to warm to room

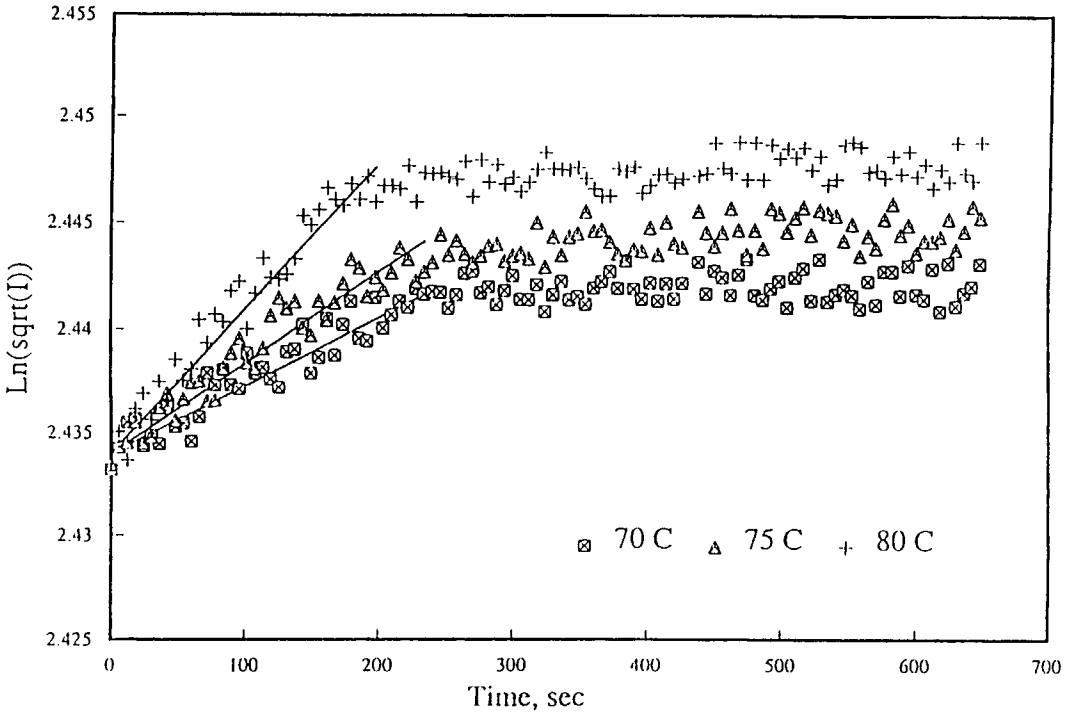

Figure 10 Plot of the natural logarithm of the square root of the intensity (at its maximum with scattering angle) of scattered light vs. time. Data corresponds to 6.75 wt % poly(methacrylic acid) in water at 70, 75, and 80°C. Straight lines adequately represent early times data, which indicates that the system phase separates via spinodal decomposition.

temperature. Then, it was placed in the light scattering cell, which was already at its operating temperature. The intensity of the photodiode array detector at 0 degree angle was measured as a function of time. Again, the sharp decrease in intensity signifies cloudiness of the mixture and the occurrence of phase separation.

To get an idea of the phase separation kinetics of the poly(methacrylic acid)-methacrylic acid–water system, we chose to study the poly(methacrylic acid)–water [number average molecular weight of poly(methacrylic acid) = 978,000 g/mol, and polydispersity index = 1.25] system using the lens and detector system shown in Figure 3. The polymer solution was prepared by charging the components in a quartz rectangular enclosure (with a path length of 1 mm) and tumble-mixing it for a few days at room temperature. The optical cell chamber (Fig. 4) was heated to its operating temperature by running hot water through it. Then, the rectangular quartz enclosure that contained the polymer solution was inserted in the heated cell chamber. Scans of intensity vs. scattering angle were taken and recorded onto a diskette.

RESULTS AND DISCUSSION

Polymerization Experiments

Figure 5 shows a plot of conversion vs. time for the polymerization of methacrylic acid through solution and FRRPP processes (error bars correspond mainly to the effects of unaccountable losses of reactor fluid). The solution polymerization system proceeds to almost 100% conversion after two hours, while the FRRPP system proceeds gradually from 80–92% conversion between two to five hours. Note that at the operating temperature of 80°C, the half-life of AIBN (used in the solution system) is 74 min,[9] and the half-life of V-50 (used in the FRRPP system) is 28 min.[10] Put in another way, after two hours, 30% of the AIBN was still undecomposed; after five hours, 0.06% of V-50 was still undecomposed. It seems that the end of the autoacceleration periods coincided with the half-lives of initiators used in the FRRPP and solution polymerization systems. However, in the solution system, this corresponds to a conversion of almost 100%, while in the FRRPP system it is about 60%.

Figure 6 shows a plot of the number average molecular weight as a function of conversion for the

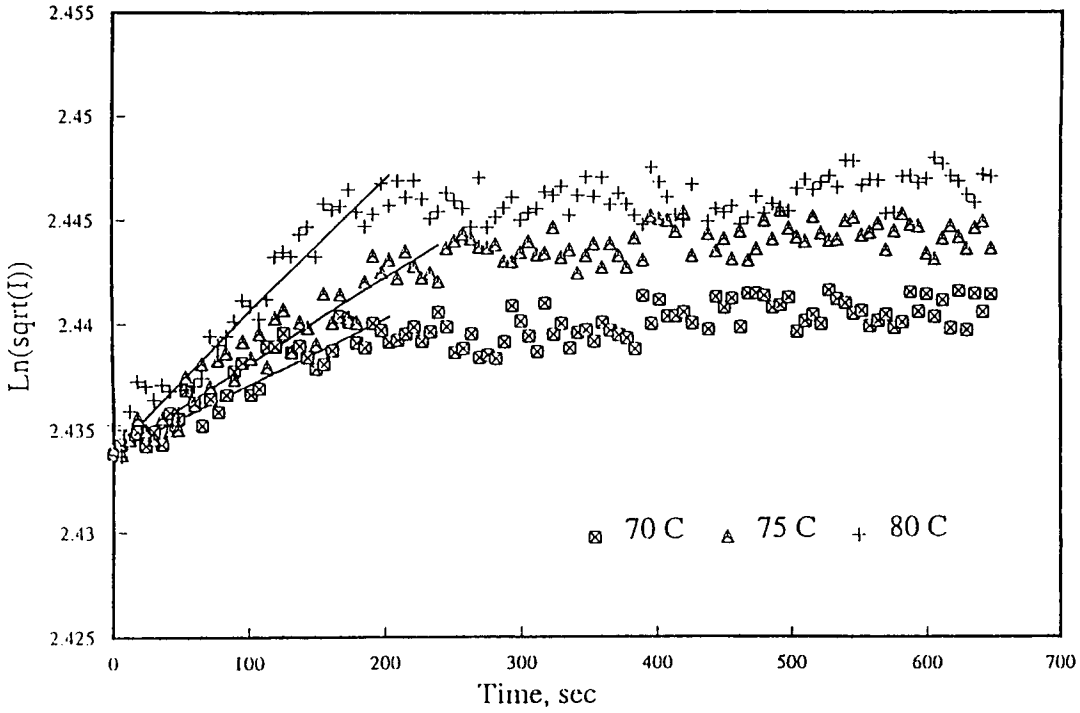

Figure 11 Plot of the natural logarithm of the square root of the intensity (at its maximum with scattering angle) of scattered light vs. time. Data corresponds to 10.53 wt % poly(methacrylic acid) in water at 70, 75, and 80°C. Straight lines adequately represent early times data, which indicates that the system phase separates via spinodal decomposition.

FRRPP and solution systems. In both systems, the number average molecular weight first increases with conversion, then it decreases and seems to asymptote to a value of about 70,000 g/mol. The increase in the number average molecular weight seems to coincide with the onset of autoacceleration, while the decrease is associated with the reduced monomer concentration. An obvious difference between the two sets of data points is that in the FRRPP system, the number average molecular weight goes to a maximum between 20–40% conversion, while it occurs between 50–70% conversion in the solution system. The maximum in the FRRPP system occurs at a number average molecular weight of about 150,000 g/mol, while it occurs at a molecular weight of about 118,000 g/mol in the solution system. This seems to indicate that the FRRPP system could have a stronger gel effect phenomenon compared to the solution system. Such observation is consistent with the relatively high conversion rate for the FRRPP system below 60% conversion (see Fig. 5). A possible explanation to this behavior is that there could be local heating around the radical site, which could lead to premature phase separation and faster decomposition of initiator molecules. As one could note in Figure 1, if the temperature of a localized region is above the LCST, then that region would be inside the phase envelope. Phase separation around the radical site will restrict its availability to terminate with another polymer radical. At these low conversions, enough monomer molecules are still available for relatively rapid radical chain propagation.

In Figure 7, a plot of the polydispersity index vs. conversion is shown for FRRPP and solution systems at 80°C. All samples showed single-peak molecular weight distributions. Also, branching was almost nonexistent in all the samples (with branching frequency of one for very molecular weight of over 100,000 g/mol). For the solution system, Figure 7 indicates that the relatively narrow molecular weight distributions were obtained at conversions below 40%. At higher conversions, the molecular weight distribution became quite broad. This broadening of the molecular weight distribution is coincident with the onset of autoacceleration. For the FRRPP system, the polydispersity index was stable between 1.5 and 1.7 at 20–92% conversion. This means that while conversion time data shows a gel effect at conversions below 60%, molecular weight control still exists.

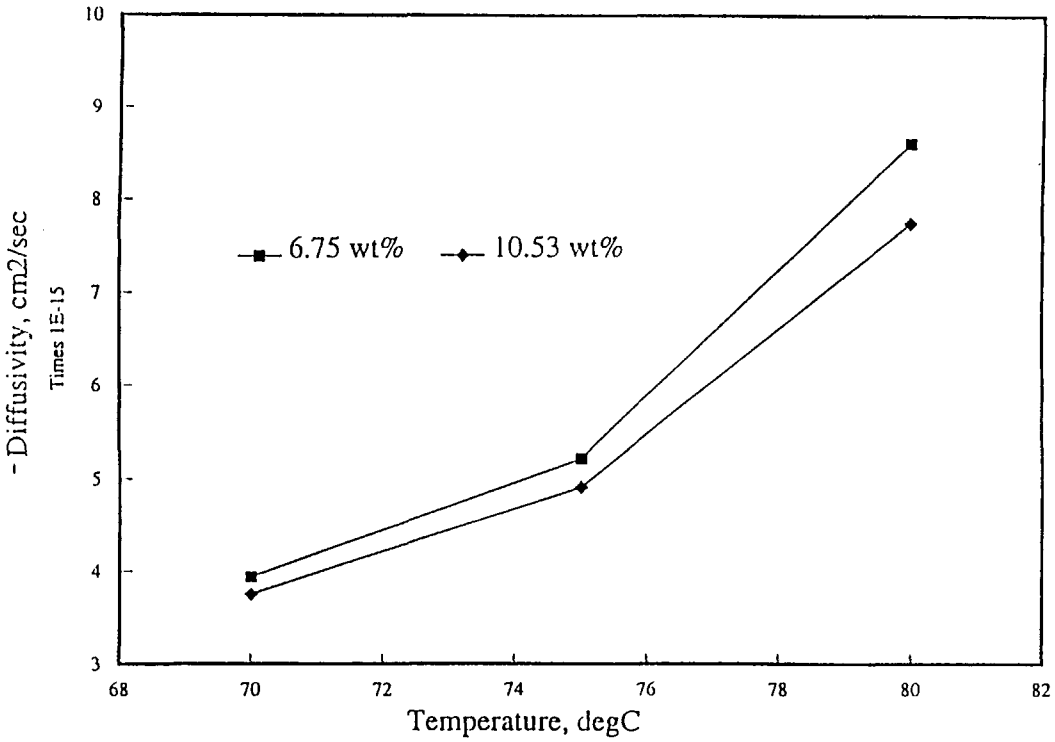

Figure 12 Plot of the negative of the diffusivity for the poly(methacrylic acid)–water system from early times data points in Figures 9 and 10. Slope values in Figures 9 and 10 were used in eqs. (1) and (2) in order to calculate the diffusivity at the indicated temperatures and polymer compositions.

Free-radical Concentration Measurements

Figure 8 shows the evolution of free-radical concentrations for polymerization of methacrylic acid under bulk, solution, conventional precipitation (CPP), and retrograde precipitation (FRRPP) conditions. The free-radical concentration is presented in the ordinate to be relative to the maximum available free-radicals coming from the initiator ($2[I]_o$), while the abscissa is in terms of the reaction time relative to the half-life of the initiator used at the operating temperature. Thus, it can be seen in Figure 8 that, for all cases, the relative free-radical concentration (ordinate value) increases at the beginning. This is understandable, since at the very beginning, the amount of initiator molecules is at its highest. As time goes by, the initiator molecules decompose into radicals based on the exponential decay behavior. If free-radicals recombine rather quickly after they are formed and propagated into polymer radicals, then the initial surge in radical concentration should be followed by an almost exponential decay behavior, ending at a relative radical concentration of almost zero at five times initiator half-life (the abscissa value is equal to 5). An obvious anomaly to this type of behavior occurs when the polymer concentration is high enough to restrict polymer radical recombination. It is therefore not a surprise to see that the solution system follows the predicted rise followed by decay of radical concentration with time. In the bulk system, the relatively high polymer concentration at high conversions results in a slower decay compared to the solution system. For the CPP system, the time evolution behavior is qualitatively the same as that of the solution system. The most interesting behavior is that of the FRRPP system, wherein the free-radical concentration goes up and stays at an asymptotic level even after almost all initiator molecules have already decomposed into radicals. Such an observation is consistent with our proposed mechanism of radical trapping in the FRRPP system.

Light Scattering Experiments

Result of cloud-point measurement is shown in Figure 9, in which the composition of phases at equilibrium is shown at a temperature range of 71–77°C. The cloud-point curve at 80°C is expected to be a

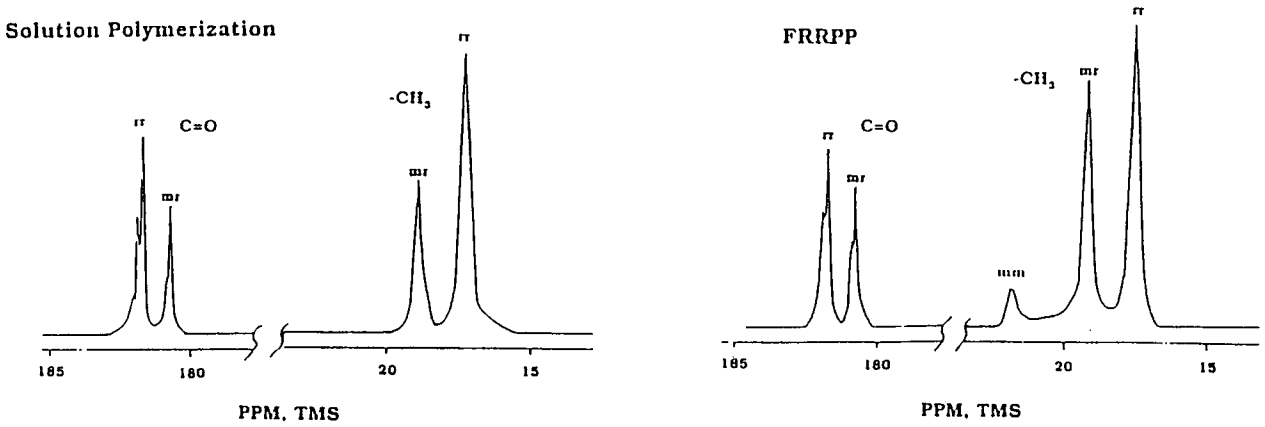

Figure 13 Portions of typical proton noise decoupled ^{13}C NMR spectra for poly(methacrylic acid) materials that were made from FRRPP and solution polymerization processes. For each carbon position in the polymer molecule, there is a maximum of three peaks due to stereoisomerism. Each of the three peaks correspond to triad configuration shown in the inset.

little larger than the phase envelope shown in the figure. Here, one can deduce from the reaction trajectory (wherein the polymer composition increases while monomer composition decreases, and solvent composition remains the same) that the system enters the phase envelope at 50–60% conversion if the reactor operating temperature is 71–77°C. At 80°C, the system would enter the phase envelope at a lower conversion because the phase envelope at this temperature is larger than that shown in Figure 9. However, as the system enters the phase envelope, it does not necessarily separate into two phases right away. The system has to cross a so-called metastable region before it enters the unstable region, where phase separation has been known to occur spontaneously[11] (a similar method of visualizing composition trajectories in ternary polymer systems is well-established in polymer membrane formation.[12]). In Figure 5, one can see that after 60% conversion the conversion rate decreases for the FRRPP system. In Figure 6, the number average molecular weight reaches an asymptote after about 60% conversion. In Figure 7 though, the polydispersity index is stable at 1.5–1.7 even at low conversions. Clearly, phase separation behavior above 60% conversion results in reduction of the polymerization rate as

Table I Relative Areas of ^{13}C Methyl ($-CH_3$) Resonances of PMAA

	Relative Areas of Triads		
Sample	rr	mr	mm
Sol. polym., 69% conv.	0.69	0.31	0.00
Sol. polym., 97% conv.	0.65	0.35	0.00
FRRPP, 74% conv.	0.54	0.38	0.08
FRRPP, 80% conv.	0.56	0.37	0.07

Table II Relative Areas of ^{13}C Carbonyl (C=O) Resonances of PMAA

	Relative Areas of Triads		
Sample	rr	mr	mm
Sol. polym., 69% conv.	0.66	0.34	0.00
Sol. polym., 97% conv.	0.72	0.28	0.00
FRRPP, 74% conv.	0.60	0.40	0.00
FRRPP, 80% conv.	0.60	0.40	0.00

Table III The Number Average Sequence Lengths (n_m and n_r) of meso and *racemic* Configurations of PMAA

	n_m		n_r	
Sample	$-CH_3$	C=O	$-CH_3$	C=O
Sol. polym., 69% conv.	1.0	1.0	5.4	4.9
Sol. polym., 97% conv.	1.0	1.0	4.7	6.1
FRRPP, 74% conv.	1.4	1.0	3.8	4.0
FRRPP, 80% conv.	1.3	1.0	3.9	4.0

well as a stable molecular weight and molecular weight distribution. The relatively narrow molecular weight distribution at conversions of 25–60% is quite unusual; it might be due to premature phase separation brought about by local heating around the radical site. This is supported by light scattering results from the reactive polymerization system inside a sealed 4-mm glass tube, which showed turbidity of the reaction mixture starting at 20–30% conversion. This *in situ* light scattering experiment was carried out at an operating temperature of 60°C, which would have an even smaller phase envelope than that in Figure 9.

Figures 10 and 11 show plots of the natural logarithm of the square root of the maximum of the intensity profile of the scattered light vs. time. Data points are shown at different temperatures for a nonreactive poly(methyl methacrylate)–water system. According to theory, the early stage of phase separation at particular temperature occurs through spinodal decomposition[13] if the data points can reasonably be represented by a straight line.[14] The slope of the straight line, $2R(q_m)$, is related to the mutual diffusivity, D, by

$$R(q_m) = -\tfrac{1}{2}(Dq_m^2) \quad (1)$$

where q_m is the wave vector, and is defined as

$$q_m = \frac{4\pi}{\lambda}\sin\left(\frac{\theta}{2}\right) \quad (2)$$

Here, λ is the wavelength of the incident laser light, while θ is the scattering angle where the maximum in intensity is occurring. Once q_m and $R(q_m)$ are known, then the mutual diffusivity, D, can be obtained from eq. 1.

Figures 10 and 11 indicate that at the early stage of phase separation, data points are reasonably represented by straight lines. In Figure 12, the negative of the diffusivity is plotted with temperature from data obtained in Figures 10 and 11, as well as from the scattering angle of the maximum in intensity profile. Clearly, from Figures 10–12, the kinetics of phase separation of poly(methacrylic acid)–water system for the overall polymer composition of 6.75 and 10.53% at 70, 75, and 80°C occur via spinodal decomposition. Other features of Figures 10–12 are consistent with observations of spinodal decomposition in other polymer systems.[14,15]

Nuclear Magnetic Resonance

Figure 13 shows typical ^{13}C NMR spectra of samples from FRRPP and solution polymerization processes. Both carbonyl (C=O) and methyl (CH_3) carbon peaks are shown. Due to stereoisomerism, three peaks (representing triads) are formed for every carbon type. The labeling of the various triads are also shown in Figure 13. For both poly(methacrylic acid) materials made from FRRPP and solution polymerization processes, the same pattern for the triad peaks are observed. For a particular poly(methacrylic acid) system, there seems to be an opposite pattern in triad peaks for carbonyl and methyl carbons. The explanation lies in the differences in the levels of shielding and deshielding of the carbons in the polymer molecule. For the methyl carbon in the rr triad, its electron cloud is shifted a little toward the adjacent carbonyl oxygen; thus, it is deshielded from the external magnetic field of the NMR spectrometer. This means that the chemical shift (ppm value) will be lower than that of the mr triad. For the carbonyl carbon in the rr triad, its electron cloud is shifted a little away from the adjacent carbonyl oxygen because the carbonyl oxygen has attracted part of the electron cloud from the adjacent methyl protons. This means that the carbonyl carbon is going to be even more shielded by its adjacent electron cloud; thus, the peak for the rr triad appears to be shifted upfield compared to the mr triad.[16]

In Tables I and II, relative areas under the peaks for the various carbons of poly(methacrylic acid) samples are indicated. As it is evident in Figure 13, it should not be surprising that Tables I and II show that the mm triad is almost nonexistent in all samples. In Table III, the relative areas of peaks from Tables I and III are used to calculate the average number of repeat unit sequences of meso and racemic diads. The ratio of the number of racemic se-

quences (n_r) to the number of meso sequences (n_m) ranges from about 3 to about 6. This means that stereoisomerism for poly(methacrylic acid) generated from FRRPP and solution polymerization processes are of random tacticity, with predominantly syndiotactic configuration. Therefore, we think that intermolecular interactions are not strong enough for the methacrylic acid molecules to align prior to reacting and affect the polymerization rate, as it was proposed to occur in acrylic acid polymerization.[17]

Based on the above-mentioned analysis of the FRRPP process, there is evidence to support the complicated physicochemical mechanism[1] outlined at the beginning of this paper. The relatively slow approach of the system to complete conversion and the relatively narrow molecular weight distributions observed in the FRRPP methacrylic acid system at 20–92% conversion are consistent with the proposed mechanism.[1] Such observation is supported by the asymptotic time behavior of the free-radical concentration (most likely due to radical trapping) even after five times the initiator half-life, when most of the initiator molecules have already decomposed.

CONCLUSIONS

We have shown in this work the occurrence of a gradual increase in conversion vs. time when a polymerization system phase separates above the lower critical solution temperature, as it was cited in our previous work. We found that the gradual increase in conversion with time roughly coincided with the entry of the system into the ternary phase envelope. For the FRRPP methacrylic acid system, the values of the polydispersity index were stable at 1.5–1.7 for a conversion range of 20–92%. Finally, time behavior of free-radical concentration for the FRRPP system showed an asymptote instead of the decay behavior that normally characteristizes free-radical polymerization systems. Such an asymptotic behavior is probably due to radical trapping, which again is consistent with our proposed mechanism for the FRRPP system.

This work has been partially supported by the Research Excellence Fund of the State of Michigan. We also acknowledge partial support of the National Science Foundation (CTS-9404156). Finally, we acknowledge Mr. Y. L. Dar for doing the sieve analysis of powdered poly(methacrylic acid) samples from the reactor experiments.

REFERENCES

1. G. T. Caneba, *Adv. Polym. Tech.*, **11**, 277 (1992).
2. C. H. Bamford, A. Ledwith, and P. K. Sen Gupta, *J. Appl. Polym. Sci.*, **25**, 2559 (1980).
3. S. K. Kumar, R. C. Reid, and U. W. Suter, *Polym. Preprints*, **27(2)**, 224 (1986).
4. M. Hoffmann, *Makromol. Chem.*, **177**, 1021 (1976).
5. G. A. Stahl and R. B. Seymour, in *Structure-Solubility Relationships in Polymer Systems*, F. W. Harris and R. B. Seymour, Eds., Academic Press, New York, 1977, pp. 259–268.
6. L. Zeman and D. Patterson, *J. Phys. Chem.*, **76**, 1214 (1972).
7. J. I. Kroschwitz, *Concise Encyclopedia of Polymer Science and Engineering*, Wiley, New York, 1990, p. 16.
8. L. J. Hughes and G. E. Britt, *J. Appl. Polym. Sci.*, **5**, 337 (1961).
9. B. M. Louie, M.S. Thesis, University of California, Berkeley, 1984, p. 32.
10. "Azo Polymerization Initiators," Product brochure for V-50 by Wako Chemicals USA, Inc., September 1987.
11. G. T. Caneba and D. S. Soong, *Macromolecules*, **18**, 2538 (1985).
12. H. Strathmann, P. Scheible, and R. W. Baker, *J. Polym. Sci.*, **15**, 811 (1971).
13. J. W. Cahn, *J. Chem. Phys.*, **42**, 93 (1965).
14. T. Hashimoto, J. Kumaki, and H. Kawai, *Macromolecules*, **16**, 641 (1983).
15. T. Izumitani and T. Hashimoto, *Macromolecules*, **83**, 1 (1985).
16. I. R. Peat and W. F. Reynolds, *Tetrahedron Lett.*, **14**, 1359 (1972).
17. A. Chapiro, "Auto-Acceleration in Free-Radical Polymerizations Under Precipitating Conditions," in *Polymer Science Overview—A Tribute to Herman F. Mark*, G. A. Stahl, Ed., ACS Symposium Series 175, 1981, pp. 233–252.

Received April 5, 1996
Accepted July 18, 1996